

Optical model analysis of scattering of 7- to 15-MeV neutrons from 1-*p* shell nuclei

J. H. Dave and C. R. Gould

North Carolina State University, Raleigh, North Carolina 27650
and Triangle Universities Nuclear Laboratory, Duke Station, Durham, North Carolina 27706

(Received 15 March 1983)

An optical model analysis of results from a program of neutron time-of-flight measurements of elastic scattering from the 1-*p* shell nuclei is described. Experiments have been carried out at the TUNL FN Tandem van de Graaff facility using the $^2\text{H}(d,n)^3\text{He}$ reaction as a neutron source. Experimental methods and past results for neutron scattering from ^6Li , ^7Li , ^9Be , ^{10}B , ^{11}B , ^{12}C , ^{13}C , and ^{16}O are summarized. Data have generally been accumulated at bombarding energies from 7 to 15 MeV in 1-MeV steps, at scattering angles from 25° to 160° . Cross sections are compared to previous work. Much of the neutron scattering data is well described by the spherical optical model, particularly for nuclei in which resonance structure is not prominent. However, spherical optical model parameters for heavier nuclei do not reproduce the data well. Parameter sets for the individual nuclei are presented along with the results of a global spherical optical model search over 45 neutron scattering angular distributions for all 1-*p* shell nuclei. Volume integrals for the real and imaginary wells are compared to recent theoretical predictions. The spherical optical model predictions for proton elastic scattering are compared to the available data for the $T=0$ nuclei. Coulomb correction terms to the real and imaginary potential well depths are investigated.

[NUCLEAR REACTIONS $^6,7\text{Li}$, ^9Be , $^{10,11}\text{B}$, $^{12,13}\text{C}$, $^{16}\text{O}(n,n)$, measured $\sigma(\theta)$,]
 $E=7-15$ MeV, deduced spherical optical model parameters.

INTRODUCTION

For medium mass and heavy nuclei, the optical model has long been known to provide an excellent phenomenological description of nucleon-nucleus elastic scattering.¹ In the past, global optical model analyses have been dominated by the generally higher accuracy charged particle data. Recently, however, the quality of neutron scattering data has begun to rival that of charged particle data, and considerable refinement in the optical model parametrizations has resulted. For example, comparisons of proton and neutron scattering data can now provide quite precise information on isospin and Coulomb corrections in the real and imaginary potential well depths.²

Although the low level density in the compound nucleus makes it questionable to apply the optical model to scattering from light nuclei ($A < 16$), it is empirically clear from proton scattering studies that optical model analysis can reproduce data for 1-*p* shell nuclei quite adequately.³ It is of interest to investigate whether any improvements can be made in these parametrizations on the basis of neutron scattering data. In the present work, we try to obtain improved global spherical optical model (SOM) parameter sets based specifically on recently obtained neutron scattering data for ^6Li and ^7Li ,⁴ ^9Be ,⁵ ^{10}B and ^{11}B ,⁶ ^{12}C ,⁷ ^{13}C ,⁸ ^{16}O ,⁹ and data for ^{14}N from Bauer *et al.*¹⁰

The new data were obtained as part of a program of measurements of cross sections for neutron elastic and discrete inelastic scattering from the 1-*p* shell nuclei. These nuclei comprise many elements of interest to fusion

reactor design studies. For example, lithium isotopes are components of the cooling and tritium breeding systems, beryllium is a neutron multiplier, and carbon, boron, and oxygen are constituents of shielding and structural materials. Energies up to 14 MeV are particularly relevant to the first generation of fusion reactors, based on the d-t reaction cycle.

The experiments covered the energy range 7–15 MeV. This is an energy region in which there have been few previous studies. The energies are below those accessible to d-t neutron generators, but above those accessible to single-ended Van de Graaff accelerators. Cross section measurements are particularly important for light nuclei because reaction models which work very well for heavier nuclei are usually much less reliable for light nuclei.

We are able to reproduce the bulk of the 1-*p* shell proton and neutron scattering data reasonably well with the SOM, particularly where resonance structure is not prominent. We have obtained energy dependent parameter sets for the individual nuclei, as well as an A dependent parameter set for all the nuclei. The fits are generally not as good as those seen for heavier nuclei. However, the parameter sets show the same qualitative trends as those seen for heavier nuclei, and indicate that the SOM is a physically reasonable way of describing the main features of elastic scattering from light nuclei.

EXPERIMENTAL PROCEDURES

The experiments have been carried out at the TUNL FN Tandem Van de Graaff neutron time-of-flight (TOF)

facility. Details specific to each of the experiments are discussed in Refs. 4–9. The samples and energies studied are listed in Table I. In general, measurements have been made at 34 angles between 25° and 160° in 1- or 2-MeV steps. Smaller energy steps were taken in regions where resonance structure was prominent in the total neutron cross section of the nucleus being studied.

Our data acquisition procedures have recently been discussed by Gould *et al.*¹¹ and El-Kadi *et al.*¹² and are only briefly summarized here. The neutron beam is produced by deuteron bombardment of a 3-cm long deuterium gas cell filled to a pressure of 2 atm. The beam current is typically 3 μ A, pulsed at a 2 MHz repetition rate and bunched to a width of about 2 ns. The scattering targets are in the form of right circular cylinders suspended vertically from a stainless steel wire a distance of 9.25 cm from the center of the gas cell. The samples were typically 2.54 cm high and 1.27 to 1.91 cm in diameter. The ${}^6\text{Li}$, ${}^7\text{Li}$, ${}^{10}\text{B}$, ${}^{11}\text{B}$, and ${}^{13}\text{C}$ samples were monoisotopic and were enclosed in thin walled aluminum cans. The ${}^9\text{Be}$ and ${}^{12}\text{C}$ samples were pure and the ${}^{16}\text{O}$ sample was in the form of BeO, enclosed between two aluminum endcaps.

The neutrons are detected by the TOF method in two heavily shielded liquid scintillators, one an 8.90 cm \times 5.08 cm NE218 scintillator at a flight path of 4 m, and the other a 12.71 cm \times 5.08 cm NE213 scintillator at a flight path of 6 m. Each detector can be placed at angles from 0° to 160° (on opposite sides of the beam) and is shielded by a tungsten metal shadow bar from the direct flux of neutrons from the gas cell. The detectors are operated at a ${}^{137}\text{Cs}$ edge bias, corresponding to a 1.9-MeV neutron cutoff. Pulse shape discrimination is used to distinguish neutron events from γ -ray events in the scintillators. A monitor NE213 detector, mounted above the scattering plane, views the gas cell directly and is used to provide a relative normalization of all the scattering data taken at a given energy. Sample out spectra were accumulated at each angle to correct for backgrounds due to scattering from the sample containers and suspension wire. For the case of oxygen, the “sample-out” spectrum was taken with a small Be sample containing the same number of beryllium atoms as the BeO sample.

The absolute normalization at each energy is obtained by comparing to hydrogen scattering from a polyethylene sample. The angular distributions obtained from the peak yields in the TOF spectra are corrected for effects due to

TABLE I. Sample masses and energies measured.

Sample	Mass (g)	Purity	Number of energies	Energy range (MeV)
${}^6\text{Li}$	3.32	94.9% ${}^6\text{Li}$	7	7.5–14
${}^7\text{Li}$	3.80	99.8% ${}^7\text{Li}$	8	7–14
${}^9\text{Be}$	13.38	99.9% ${}^9\text{Be}$	9	7–15
${}^{10}\text{B}$	8.65	92.4% ${}^{10}\text{B}$	7	8–14
${}^{11}\text{B}$	8.87	97.1% ${}^{11}\text{B}$	8	8–14
${}^{12}\text{C}$	12.50	natural C	16	9–15
${}^{13}\text{C}$	8.53	99% ${}^{13}\text{C}$	5	10–18
${}^{16}\text{O}$	19.19	natural BeO	11	9.2–15

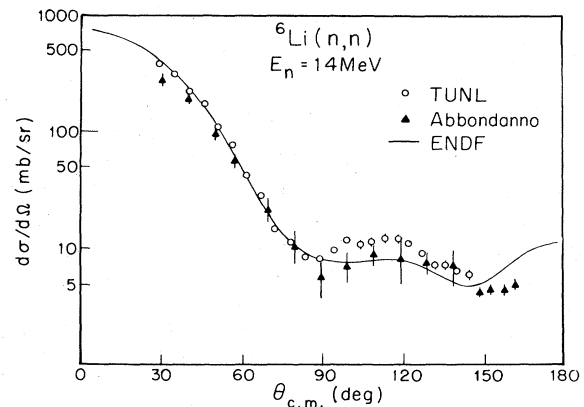


FIG. 1. Differential cross sections for ${}^6\text{Li}(n,n)$ from the present work compared to the results of Ref. 15 and the current ENDF evaluation (Ref. 16).

the extended neutron source, the finite sample size, and the finite detector size. These corrections are carried out using Monte Carlo simulation. The code calculates a neutron TOF spectrum at each angle, based on the experimental geometry and input libraries of cross sections versus energy for all elements in the sample. The code can handle one or two element samples, as in the case of the oxygen scattering data. The code can take energy loss following elastic scattering into account. This proves to be an important correction in multiple scattering of neutrons from light elements because the energy loss can have the effect of removing the scattered neutrons from the TOF peak of interest. A few iterations are sufficient to reach agreement between the calculated and measured peak yields in the TOF spectra. We estimate our total elastic cross sections to be good to about 5% at the higher energies, with somewhat smaller errors at the lower energies.

Below 14 MeV there are relatively few experiments with which we can compare our results. An exception is the carbon data set from 8.0 to 14.5 MeV of Haouat *et al.*¹³

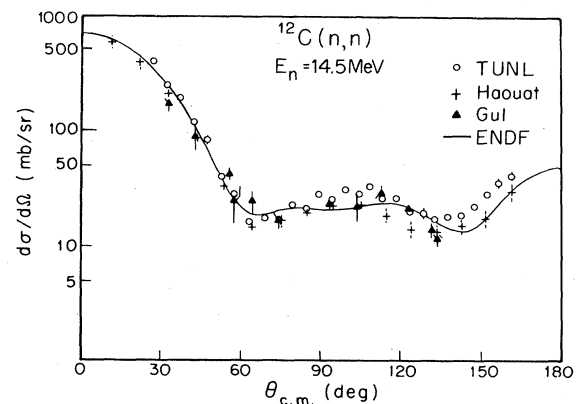


FIG. 2. Differential cross sections for ${}^{12}\text{C}(n,n)$ from the present work compared to the results of Refs. 13 and 17 and the current ENDF evaluation (Ref. 18).

We see good agreement with their work, except at 14.0 and 14.5 MeV where our cross section results are systematically higher. Above 14 MeV there have been a number of studies of neutron scattering using the d-t reaction as a neutron source, and the ENDF evaluations¹⁴ rely heavily on these measurements. As examples, Fig. 1 shows our ${}^6\text{Li}$ results compared to the measurements of Abbondanno *et al.*¹⁵ and the current ENDF evaluation,¹⁶ and Fig. 2 shows our ${}^{12}\text{C}$ results at 14.5 MeV compared to the results of Haouat *et al.*,¹³ Gul *et al.*,¹⁷ and the ENDF evaluation.¹⁸ In general, our results at around 14 MeV show reasonable agreement with the ENDF evaluation at forward angles but possible systematic discrepancies at back angles and in deep diffraction minima.¹¹

The final data from these experiments are available upon request from the National Nuclear Data Center (NNDC) and in two cases differ from our previously published results. Improvements in the multiple scattering codes were made after the ${}^{12}\text{C}$ measurements, and the NNDC ${}^{12}\text{C}$ data set supersedes that originally published in Ref. 7. Also, the cross sections and Legendre polynomial coefficients for elastic scattering from ${}^{11}\text{B}$ are incorrectly interchanged in Ref. 6 for 9.69 and 9.96 MeV. It should be noted that inelastic scattering to the 0.478 MeV state in ${}^7\text{Li}$ was not resolved from elastic scattering in our experiment. For the optical model analysis presented here, an assumed isotropic contribution from this state was subtracted out (see Ref. 4).

OPTICAL MODEL FITS TO NEUTRON DATA

SOM fits have been made to the elastic scattering angular distributions using the code GENOA.¹⁹ Many of the 1-*p* shell nuclei are nonspherical, but it is known that deformation effects can be masked by suitable choices of SOM

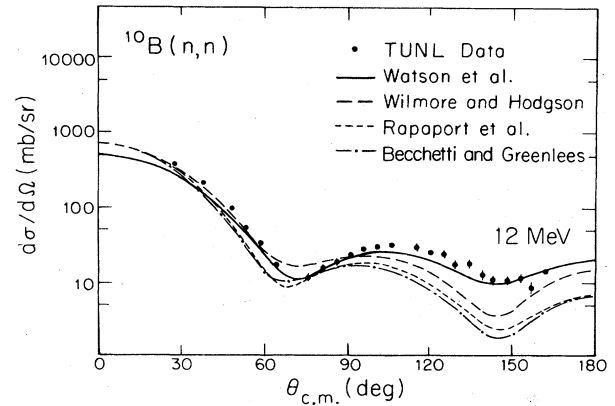


FIG. 3. Measured angular distribution for elastic scattering of 12 MeV neutrons from ${}^{10}\text{B}$, and SOM predictions using the parameters from Refs. 3 and 21–23. Disagreements indicate that optical model parameter sets based on fits to proton data, or fits to data for heavier nuclei, do not, in general, reproduce neutron scattering data from light nuclei.

parameters.²⁰ Resonance structure cannot, of course, be fit by the optical model, and we have focused on fitting the general trends of the data rather than seeking the best fit at each energy for every nucleus.

We first investigated how well standard SOM parameter sets would fit the cross section results. A comparison is shown in Fig. 3 for ${}^{10}\text{B}$ neutron scattering at 12 MeV. The Becchetti and Greenlees parameters²¹ are based primarily on proton data, while the Wilmore and Hodgson²² and Rapoport²³ parameters are specifically for neutron data. They are all parameter sets which reproduce scattering cross sections well for medium mass and heavy nuclei. The agreement with the measured ${}^{10}\text{B}$ data is not good,

TABLE II. Spherical optical model parameters for neutron scattering from 1-*p* shell nuclei (potentials in MeV, radii in fm, and c.m. energy *E* in MeV). The potential is of the form

$$U_{\text{opt}} = -V_0 f(r, r_0, a_0) + 4i a_i W_d \frac{df}{dr}(r, r_i, a_i) + 2V_{\text{so}} \frac{\sigma \cdot \mathbf{I}}{r} \frac{df}{dr}(r, r_{\text{so}}, a_{\text{so}}),$$

where *f* is the usual Wood-Saxon form factor

$$f(r, r_x, a_x) = [1 + \exp(r - r_x A^{1/3})/a_x]^{-1}.$$

	V_0	r_0	a_0	W_d	r_i	a_i	V_{so}	r_{so}	a_{so}
${}^6\text{Li}$	39.62−0.027 <i>E</i>	1.507	0.663	9.298+0.646 <i>E</i>	1.616	0.196	5.5	1.15	0.5
${}^7\text{Li}$	37.74−0.001 <i>E</i>	1.504	0.565	0.165+1.113 <i>E</i>	1.512	0.185	5.5	1.15	0.5
${}^9\text{Be}$	38.50−0.145 <i>E</i>	1.447	0.387	1.666+0.365 <i>E</i>	1.368	0.424	5.5	1.15	0.5
${}^{10}\text{B}$	47.91−0.346 <i>E</i>	1.387	0.464	0.657+0.810 <i>E</i>	1.336	0.278	5.5	1.15	0.5
${}^{11}\text{B}$	45.66−0.004 <i>E</i>	1.337	0.548	0.003+1.219 <i>E</i>	1.438	0.182	5.5	1.15	0.5
${}^{12}\text{C}$	58.86−0.663 <i>E</i>	1.211	0.434	12.65+0.045 <i>E</i>	1.387	0.163	5.5	1.15	0.5
${}^{13}\text{C}$	61.23−0.765 <i>E</i>	1.131	0.561	16.40+0.136 <i>E</i>	1.412	0.112	5.5	1.15	0.5
${}^{14}\text{N}$	50.54−0.006 <i>E</i>	1.209	0.573	12.07+0.703 <i>E</i>	1.415	0.105	5.5	1.15	0.5
${}^{16}\text{O}$	48.25−0.053 <i>E</i>	1.255	0.536	4.418+0.556 <i>E</i>	1.352	0.205	5.5	1.15	0.5
Global	45.14−0.020 <i>E</i>	1.508	0.5	11.32+0.237 <i>E</i>	1.353	0.200	5.5	1.15	0.5
	−23.48 $\frac{(N-Z)}{A}$	0.0133 <i>A</i>		−16.08 $\frac{(N-Z)}{A}$					

however. The Watson parameters,³ although based mostly on fits to proton data, were specifically for light nuclei and do in fact reproduce the data somewhat better than the other sets. There is still room for improvement though, and we proceeded to search for global SOM parameter sets based specifically on neutron scattering data.

The searches used a potential of the standard form, having a Woods-Saxon real volume term and surface derivative imaginary and spin orbit terms. The form of the potential is listed in Table II. The data are from the present work except those for ¹⁴N, which are from Bauer *et al.*¹⁰ Compound nucleus contributions are discussed further in a later section and are not included here.

Polarization data were not considered in the present work and the spin orbit parameters were fixed early in the search at close to standard values.^{3,20} The value of Wick's limit was included as a data point at zero degrees. It was assigned an error of 10%. Although Wick's limit is only a lower limit on the zero degree cross section, it is known to predict the cross section fairly accurately for heavier nuclei, and for light nuclei where resonant structure is absent.²⁴

Searches were first made for individual nuclei, taking into account the known ambiguities in Vr^2 and Wa . We

allowed the real and imaginary well depths to vary linearly with energy, but did not include energy dependence in the geometric parameters. The parameters obtained in these fits are listed in Table II. The fits are shown in Fig. 4 as the dashed lines.

The parameters for the different nuclei are similar except for r_0 , which decreases with increasing A . A second search was therefore attempted over all the nuclei except nitrogen, using as starting parameters the average values from the individual searches. For this search, called a global search, a dependence of the radius parameter r_0 on the mass number A was used. Such a dependence has been used by Rapaport *et al.*²³ for heavy nuclei. In contrast to these authors we find r_0 has to be decreasing linearly with A for light nuclei. The fits obtained with this global parameter set are shown as the solid lines in Fig. 4. The parameters are listed under global in Table II.

Figure 5 shows the total and reaction cross sections from 6 to 20 MeV compared to the predictions of the optical model parameter sets found here. The data are the solid lines and are from ENDF/B-V for all nuclei except ¹³C. For ¹³C the total cross sections are from Auchampaugh *et al.*²⁵ and there are no reaction cross section data. The experimental reaction cross section plotted here is the

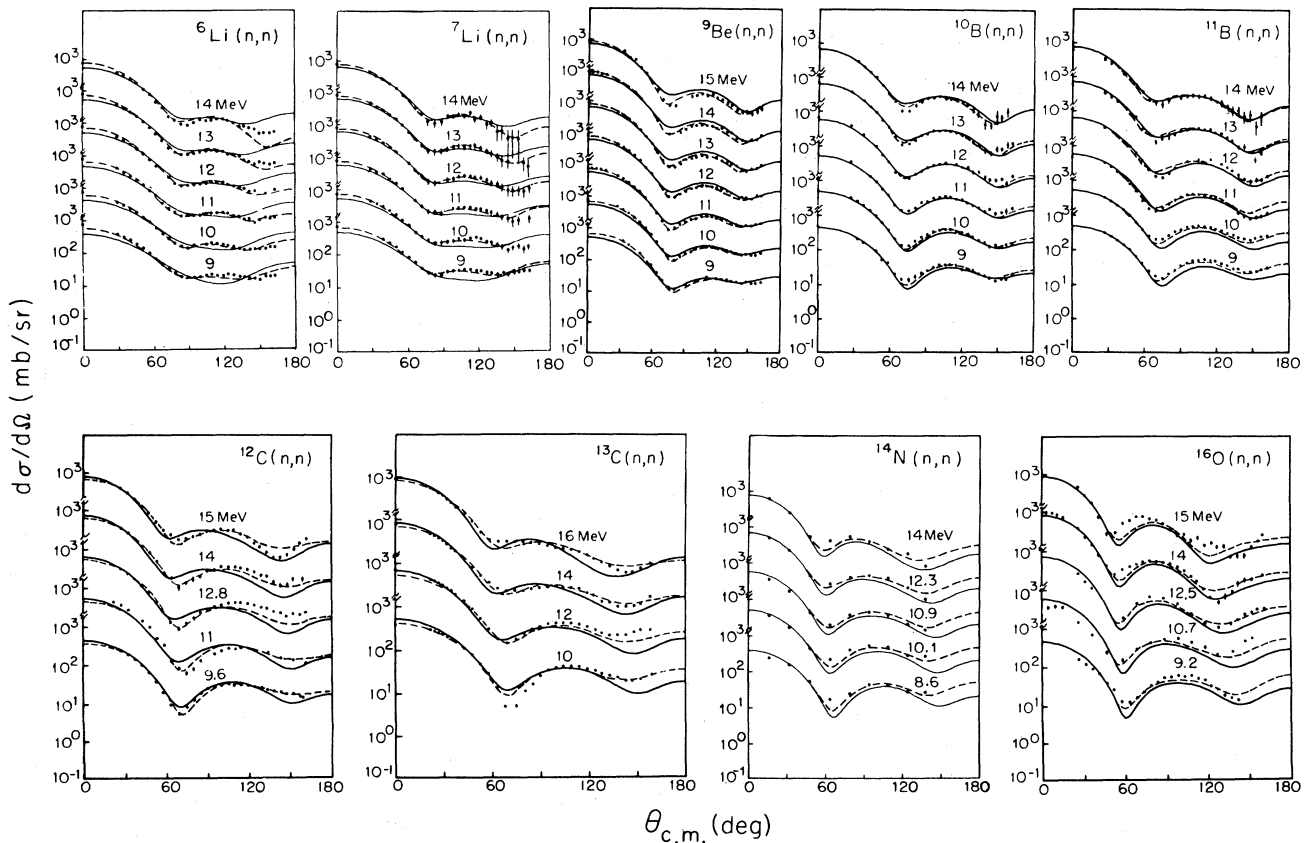


FIG. 4. Neutron elastic scattering angular distributions compared to SOM predictions based on the parameters of Table II. Data are from the present work except for ¹⁴N, which are from Bauer *et al.* (Ref. 10). Dotted lines are for the individual parameter sets, solid lines are for the global parameter set, having an A dependent real well radius parameter r_0 . The best fits are for the lighter nuclei where resonant structure in the total cross section is not prominent (see Fig. 5).

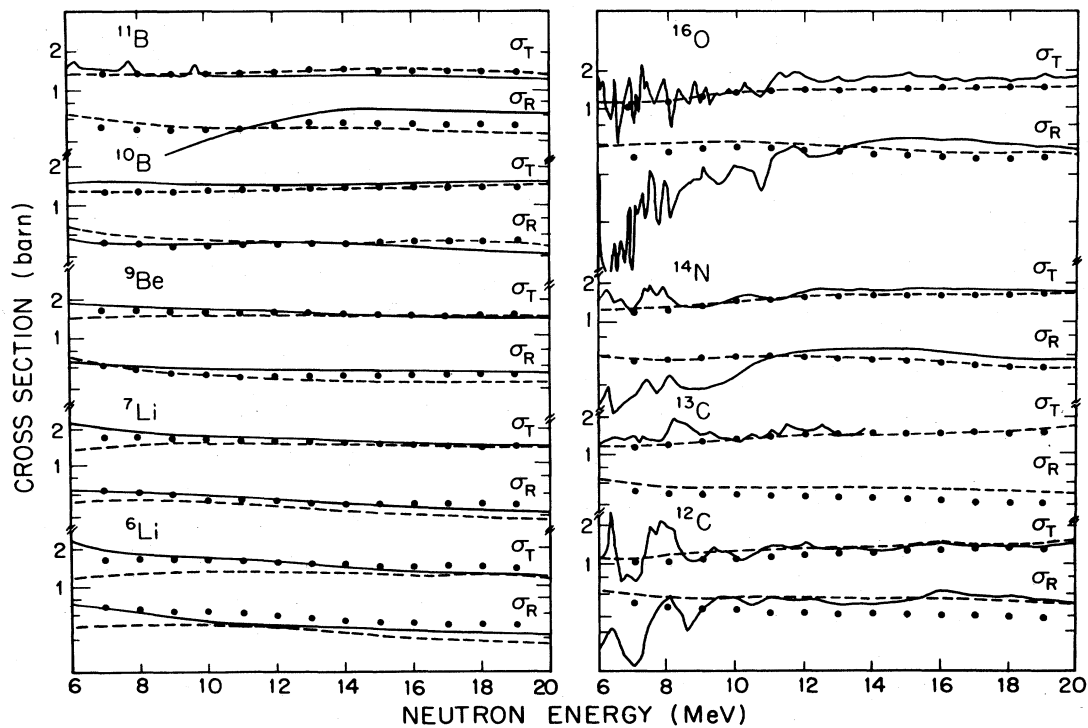


FIG. 5. Total and reaction cross sections (solid lines) compared to SOM predictions based on the parameters of Table II (points for the global parameter set and dashed lines for the individual parameter sets). Data are from Ref. 14 except for ^{13}C (Ref. 25).

nonelastic cross section and does not include any compound elastic scattering cross section. The SOM calculations (points for the global parameter set, dotted lines for the individual parameter sets) show the absorption cross sections which do include compound nucleus processes. The absorption and nonelastic cross sections are the same

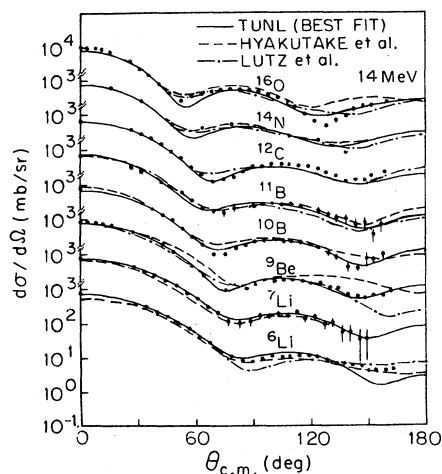


FIG. 6. Neutron cross sections at 14 MeV and individual SOM predictions from the present work compared to the SOM predictions of Lutz *et al.* (Ref. 26) and of Hyakutake *et al.* (Ref. 27). Both groups found the real well radius parameter, r_0 , to be decreasing with increasing A , as in the present work.

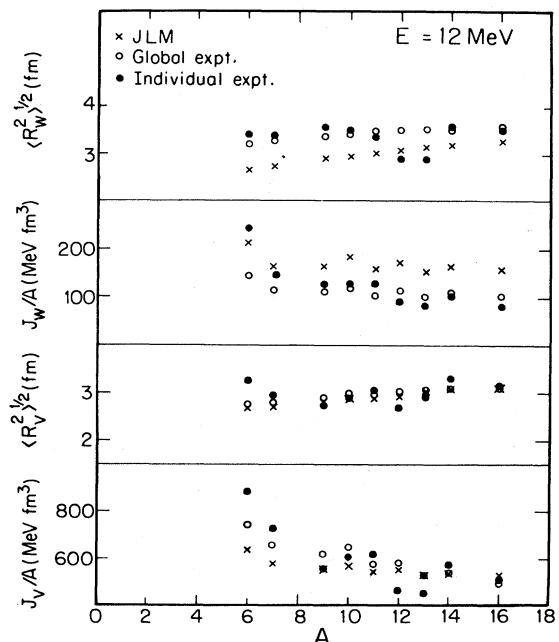


FIG. 7. Volume integrals and root mean square radii for the real and imaginary wells of the optical potentials found in the present work for 12 MeV neutrons. The values are compared to the theoretical values of Jeukenne *et al.* (Ref. 28), labeled JLM. In general, the values calculated from the global parameter set are closer to JLM than those calculated from the individual parameter sets, and better reproduce the expected trend with increasing A . Imaginary well values are systematically off.

only in as much as compound nuclear processes are negligible.

The best fits to the angular distributions and total cross sections are obtained for the lighter nuclei ($A < 11$). For carbon, nitrogen, and oxygen, resonance structure is much more prominent in the total cross sections and the fits are, as expected, somewhat poorer.

The only other systematic SOM searches over 1- p shell neutron scattering data have been those of Lutz *et al.*²⁶ and of Hyakutake *et al.*²⁷ Both searches were confined to the single energy 14 MeV and both used a Gaussian imaginary well form factor as opposed to a surface derivative term. Their parameters reproduce our data quite well, however. This is seen in Fig. 6, which shows our data and individual SOM predictions at 14 MeV, along with the individual SOM predictions of Ref. 26 and parameter set S in Ref. 27. Both authors found global parameter sets in which r_0 decreased with increasing A , as in the present work.

Volume integrals are a convenient way of comparing different optical model parameter sets. Jeukenne *et al.*²⁸ have recently made extensive calculations of root mean square radii and volume integrals of optical potentials. While these would not necessarily be expected to be appropriate for light nuclei, it is interesting to compare their predictions with the values obtained from the parameter sets found in the present work. Figure 7 shows this comparison for 12 MeV neutrons for the individual and global parameter sets as a function of mass number A . The calculated values from Ref. 28 (called JLM) are marked with crosses. The J/A are the volume integrals per nucleon for the real (V) and imaginary (W) wells. The other values are the root mean square radii, also for the real and imaginary wells. Overall trends with A are reproduced. The values calculated from the global parameter set (open circles) are closer to the JLM values than those from the individually optimized SOM parameter sets (closed circles). The differences between global and individual sets are greatest

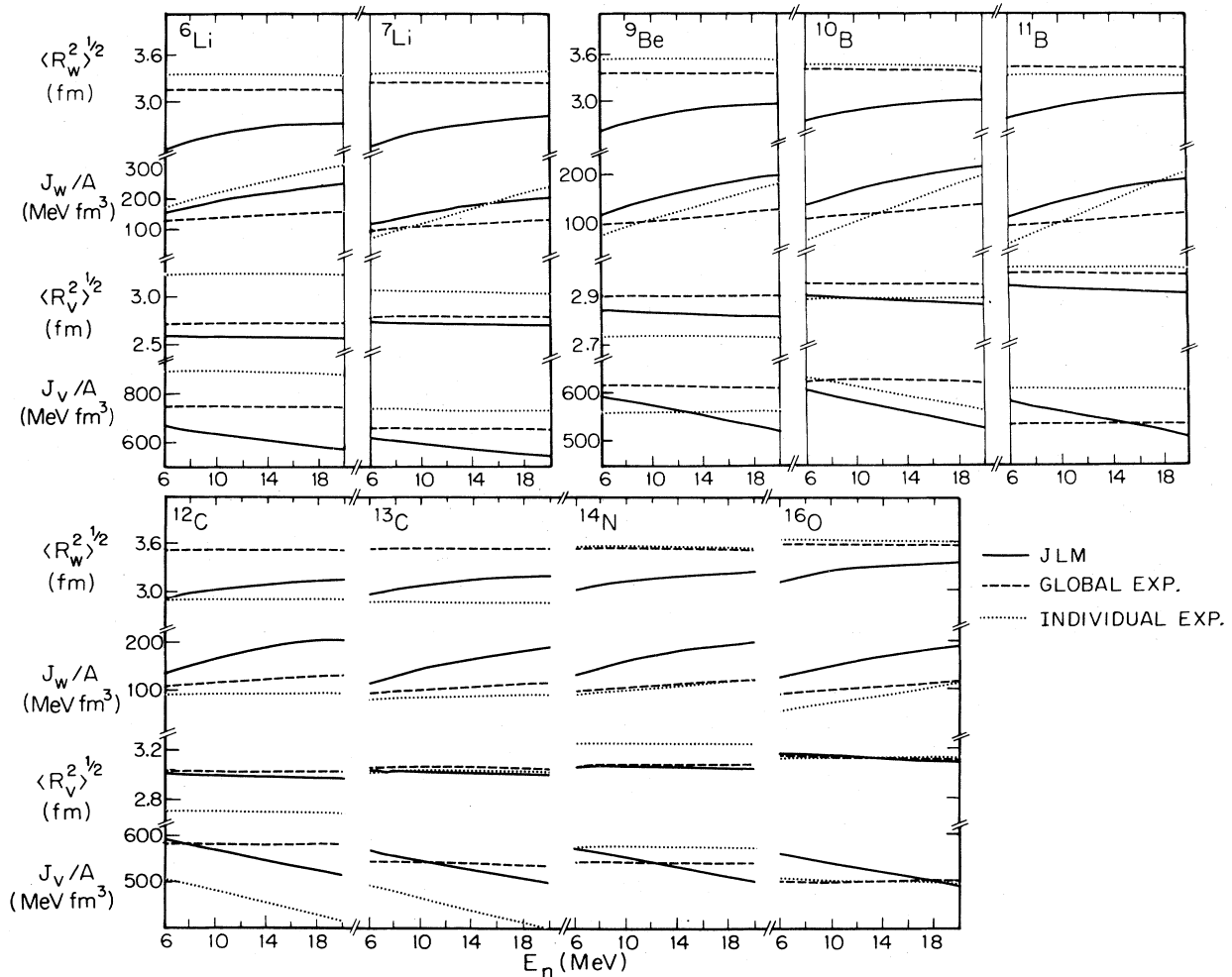


FIG. 8. Volume integrals and root mean square radii as a function of neutron bombarding energy for each nucleus studied in the present work. The energy dependences of the real well volume integrals are generally much weaker than that of JLM, while those of the imaginary well are more comparable to JLM.

for the lithium and carbon isotopes. The integrals and radii for the imaginary well are systematically off for nearly all the nuclei. This confirms difficulties previously noted in connection with the fact that the local density approximation is a much more drastic simplification for light nuclei than for heavy nuclei.²⁹ Disagreements here reflect the fact that light nuclei, while exhibiting scattering behavior similar to heavier nuclei, need to be considered separately as regards the determination of general trends in SOM parameter sets.

The energy dependences of the potentials found in the present work are more clearly summarized in Fig. 8. This shows the volume integrals and rms radii for each nucleus as a function of energy, again compared to the JLM values. The fits were made over a relatively restricted range of energies; however, the energy dependences are physically reasonable. The real well depths decrease with energy while the imaginary well depths increase with energy. There are indications in the literature^{30,31} that the energy dependence of the real well should decrease with increasing A . This is not confirmed by the global parameter set found in the present work, which shows a much weaker dependence on energy than that of the JLM real well volume integrals. Three of the individual parameter sets (^{10}B , ^{12}C , ^{13}C) show an energy dependence comparable to JLM and two of these (^{12}C , ^{13}C) clearly give better fits to the experimental data than the global parameter set. The energy dependence of the imaginary well depth of the global parameter set is reasonably consistent with JLM, while those of the individual parameter sets vary around this average value. Unique energy dependences should probably not be expected, as specifically A -dependent effects, for example associated with the actual excitation spectrum of the nucleus, will be quite important at these low energies, particularly for the imaginary well.³²

OPTICAL MODEL FITS TO PROTON DATA

We can assess the usefulness of the neutron SOM parameter sets obtained here by seeing how well they predict proton scattering data for the same nuclei. For the $T=0$ nuclei (^6Li , ^{10}B , ^{12}C , ^{14}N , and ^{16}O) the comparison is particularly straightforward. The only change in the parameters should arise from Coulomb correction terms in the real and imaginary well depths. Isospin dependent terms will necessarily be zero. Coulomb correction terms arise from the energy dependences of the well depths. Since V and W are energy dependent, we expect correction terms ΔV and ΔW in both the real and imaginary well depths, respectively.

The SOM searches have been made for the proton data of Harrison and Whitehead³³ for ^6Li , Watson *et al.*³ for ^{10}B , Daehnick and Sherr³⁴ for ^{12}C , Hansen *et al.*³⁵ for ^{14}N , and Hiddleston *et al.*³⁶ for ^{16}O . In the first search the individual parameters of Table II were used, but V and W were allowed to vary. (The Coulomb radius was set equal to the real well radius.) The results of this search are shown as the dotted lines in Fig. 9. The fits are quite

good. The resulting differences in the proton and neutron potentials ΔV and ΔW are plotted in Fig. 10. These are the Coulomb correction terms for light nuclei. The dotted lines are predictions of Rapaport³⁷ based on a study of scattering data from heavier $T=0$ nuclei. Rapaport's imaginary well correction term includes a slight energy dependence, and the values in Fig. 10 are calculated for 12-MeV neutrons. A clear pattern in our values is not discernible because of the large errors. However, the values found for the light nuclei are not necessarily inconsistent with those found for heavier nuclei.

In the second search we used our global neutron parameter set and fixed the Coulomb correction terms at standard values $\Delta V=0.4Z/A^{1/3}$ and $\Delta W=0$. The results of this fit are shown as the solid lines in Fig. 9. The agreement here is quite poor, particularly for ^{14}N and ^{16}O . In looking at Fig. 10, it is clear that the discrepancies for these two nuclei are associated primarily with setting $\Delta W=0$. Based on these results we see that we are able to fit neutron and proton scattering data from light nuclei quite well as long as Coulomb correction terms are included for both the real and imaginary well depths. However, nuclear structure effects appear to be too strong to allow us to draw any definite conclusions about a systematic ΔW term.

COMPOUND NUCLEAR CROSS SECTION CALCULATIONS

Compound nuclear (CN) contributions to the elastic scattering cross sections were calculated with the Hauser-Feshbach equation using the code HAUSER*5.³⁸ Hauser-Feshbach (HF) calculations are expected to be less accurate for light nuclei than for heavy nuclei for a number of reasons. First, the level densities are too low to allow the use of analytic expressions. Discrete level information must be used, and the calculations are then quite sensitive to the reliability of the level schemes for each nucleus involved. Second, the optical model parameters used to calculate the transmission coefficients are not as reliably determined as those for heavier nuclei, particularly for α particle emission channels. Third, direct multiparticle breakup can be important for very light nuclei. This process, in contrast to sequential breakup, is not taken into account in the HF formalism. Finally, the equations for calculating cross sections are based on transmission coefficients derived from smoothly varying optical model potentials and cannot be used to fit the resonance structure that occurs for many of these nuclei. As a result, the calculations are expected to provide only gross upper limit to the CN contributions.

The method of calculation was analogous to that used by Hansen *et al.*³⁵ in estimating CN contributions to $^{14}\text{N}(p,p)$ scattering. All energetically accessible two body breakup channels were taken into account. The level schemes in the Lederer and Shirley compilations³⁹ were used in place of analytic level density expressions. The optical model parameters for neutrons and protons were taken from the global parameter set found in the present

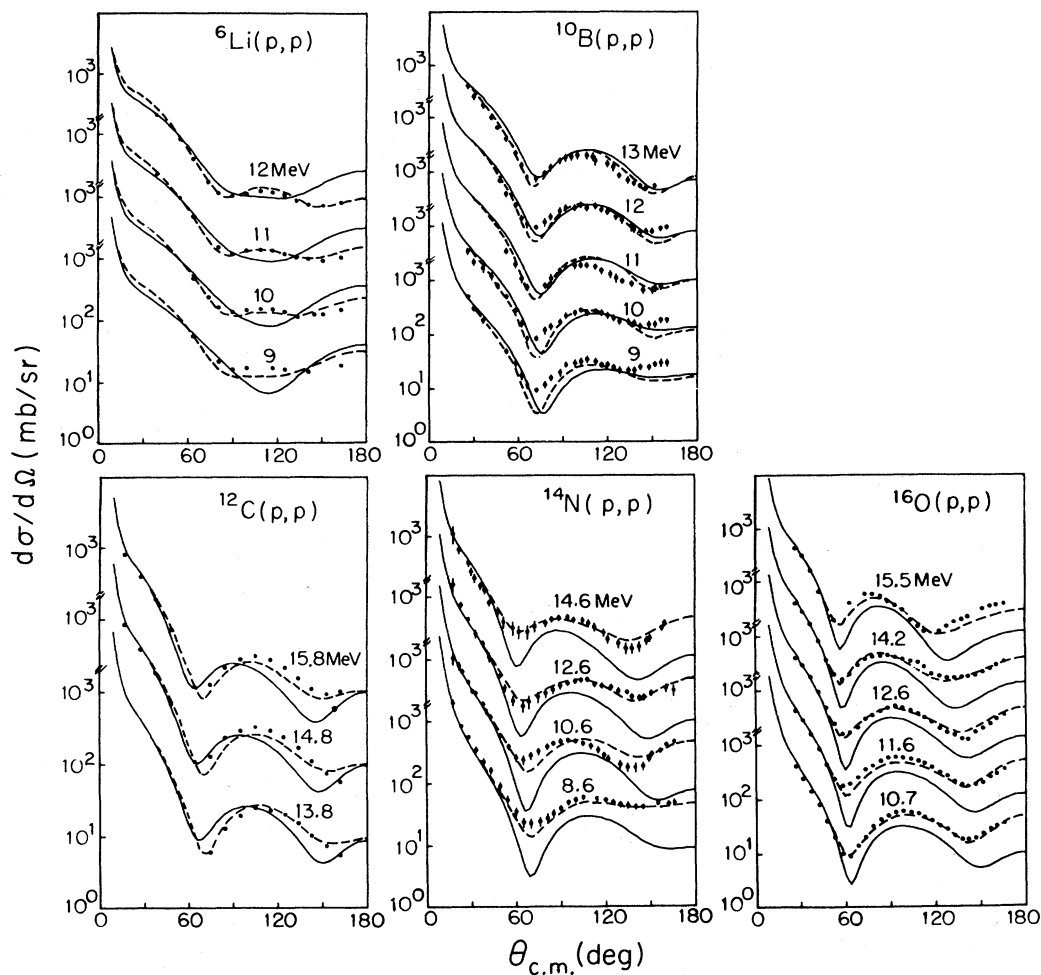


FIG. 9. Proton elastic scattering angular distributions for $T=0$ nuclei compared to SOM predictions based on the neutron parameter sets. Dotted lines are for the individual parameter sets allowing V and W to vary. The solid line is for the global parameter set including a fixed Coulomb correction term for the real well and a correction term of zero for the imaginary well (see text). The data are from Ref. 33 for ${}^6\text{Li}$, Ref. 3 for ${}^{10}\text{B}$, Ref. 34 for ${}^{12}\text{C}$, Ref. 35 for ${}^{14}\text{N}$, and Ref. 36 for ${}^{16}\text{O}$.

work. The sign of the isospin term in Table II was reversed for protons. For the other particles, α , d , t , and ${}^3\text{He}$, the default parameters from HAUSER⁵ were used. Calculations were made both with and without width fluctuation corrections.⁴⁰ The effect of the width fluctuation corrections was to raise the total CN elastic cross sections by, on the average, a factor of 2.

The dashed lines in Fig. 11 show the calculated CN cross sections, including width fluctuation corrections, for ${}^{10}\text{B}$ proton and neutron scattering at 12 MeV. The circles are the experimental data corrected for the CN contribution and the crosses are the uncorrected data. The solid lines are SOM calculations obtained with the individual parameter sets of the present work.

The CN contribution has only a small effect on the neutron distribution. The CN contribution to the proton scattering data appears to be larger, although the fit in the

forward angle minimum is actually improved compared to the uncorrected data. Zwiegliniski *et al.*⁴¹ also analyzed proton scattering data from ${}^{10}\text{B}$ and concluded that the HF calculations were significantly overestimating the CN contributions. They introduced an empirically determined reduction coefficient of average value 0.58 to scale down the HF cross section values. A similar reduction of our HF cross sections would have the effect of making the CN contributions negligible for both the proton as well as the neutron data.

We conclude that there are small CN contributions to the elastic scattering distributions, and that the corrections are difficult to calculate reliably for these light nuclei. In view of the uncertainties in calculating these contributions, we have chosen to analyze the data without first subtracting HF corrections. The SOM parameters we have determined will, to a certain extent, mask these

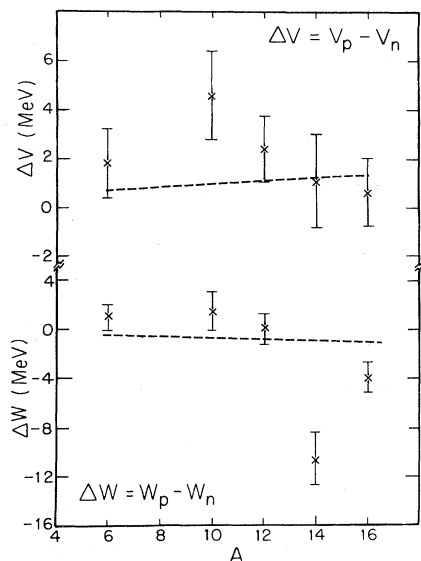


FIG. 10. Coulomb correction terms for light nuclei based on fits to the proton data of Fig. 7. The dotted lines are the predicted values of Rapaport (Ref. 37). Both real and imaginary Coulomb corrections are needed to fit the proton data; however, clearcut systematics in these terms appear to be masked by nuclear structure effects.

CN effects. The parameters will not depend on the explicit details of the HF calculation, however. The corrections are likely to be more significant in the analysis of inelastic scattering cross sections and should be included in, for example, coupled channel analysis of neutron elastic and inelastic scattering data.

SUMMARY

We have reviewed a program of measurements of neutron elastic scattering cross sections for 1-*p* shell nuclei. Data have been accumulated for neutrons in the energy range 7–15 MeV and have been compared to SOM predictions. Energy dependent parameter sets have been obtained for individual nuclei and provide a good description of the main features of the scattering distributions. A global parameter set containing an *A* dependent real well radius parameter has also been found. The best fits are obtained for the lithium and boron isotopes, and beryllium. We have compared our volume integrals and root

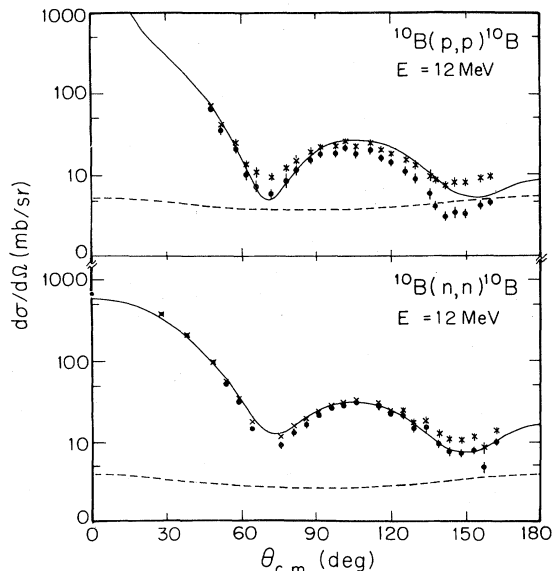


FIG. 11. Compound nuclear contributions to proton and neutron elastic scattering at 12 MeV from ^{10}B compared to the experimental angular distributions. The circles are the experimental data corrected for the CN contribution and the crosses are the uncorrected data. The solid lines are the fits obtained with the individual SOM parameter sets and the dashed lines are the calculated CN contributions.

mean square radii to recent theoretical predictions. Qualitative trends are reproduced but the imaginary well parameters are systematically off. By including real and imaginary Coulomb correction terms with the individual neutron parameters, we can fit proton scattering data for $T=0$ nuclei. Clearcut systematics in these correction terms are not evident, however, presumably due to strong nuclear structure effects. Overall, the SOM describes the bulk of neutron and proton scattering data in the 7 to 15 MeV energy range quite satisfactorily.

ACKNOWLEDGMENTS

We would like to thank the past and present members of the TUNL neutron scattering group for their invaluable help and contributions to the experiment discussed here. This work was supported in part by the U.S. Department of Energy.

¹P. E. Hodgson, *Nuclear Reactions and Nuclear Structure* (Clarendon, Oxford, 1971).

²J. Rapaport, *Phys. Rep.* **87**, 25 (1982).

³B. A. Watson, P. P. Singh, and R. E. Segel, *Phys. Rev.* **182**, 977 (1969).

⁴H. H. Hogue *et al.*, *Nucl. Sci. Eng.* **69**, 22 (1979).

⁵H. H. Hogue *et al.*, *Nucl. Sci. Eng.* **68**, 38 (1978).

⁶S. G. Glendinning *et al.*, *Nucl. Sci. Eng.* **80**, 256 (1982).

⁷D. G. Glasgow *et al.*, *Nucl. Sci. Eng.* **61**, 521 (1976).

⁸J. H. Dave *et al.*, *Nucl. Sci. Eng.* **80**, 388 (1982).

⁹S. G. Glendinning *et al.*, *Nucl. Sci. Eng.* **82**, 393 (1982).

¹⁰R. W. Bauer *et al.*, *Nucl. Phys.* **A93**, 673 (1967).

¹¹C. R. Gould, J. Dave, and R. L. Walter, in *Proceedings of the International Conference on Nuclear Data for Science and*

- Technology, Antwerp, 1982*, edited by K. H. Bockhoff (Reidel, Dordrecht, 1983), p. 766.
- ¹²S. M. El-Kadi *et al.*, Nucl. Phys. A390, 509 (1982).
- ¹³G. Haouat *et al.*, Nucl. Sci. Eng. 65, 331 (1978).
- ¹⁴ENDF/B Summary Documentation, BNL-NCS-17541 (ENDF-201), 3rd ed. (ENDF/B-V), 1979, edited by R. Kinsey, available from National Nuclear Data Center, Brookhaven National Laboratory, Upton, NY.
- ¹⁵U. Abbondanno *et al.*, Nuovo Cimento 66, 139 (1970).
- ¹⁶ENDF/B-V data file for ⁶Li (MAT 1303), evaluation by G. Hale, L. Stewart, and P. G. Young, Los Alamos National Laboratory Report No. LA-7663-MS, 1978.
- ¹⁷K. Gul *et al.*, Phys. Rev. C 24, 2456 (1981).
- ¹⁸ENDF/B-V data file for ¹²C (MAT 1306) evaluation by C. Y. Fu and F. G. Perey, At. Data Nucl. Data Tables 22, 249 (1978).
- ¹⁹F. Perey (private communication).
- ²⁰H. J. Votava, T. B. Clegg, E. J. Ludwig, and W. J. Thompson, Nucl. Phys. A204, 529 (1973).
- ²¹F. D. Becchetti and G. W. Greenlees, Phys. Rev. 182, 1190 (1969).
- ²²D. Wilmore and P. E. Hodgson, Nucl. Phys. 55, 673 (1964).
- ²³J. Rapaport, V. Kulkarni, and R. W. Finlay, Nucl. Phys. A330, 15 (1979).
- ²⁴W. P. Bucher *et al.*, Nucl. Sci. Eng. 54, 416 (1974).
- ²⁵G. F. Auchampaugh, S. Plattard, and N. W. Hill, Nucl. Sci. Eng. 69, 30 (1979).
- ²⁶H. F. Lutz, J. B. Mason, and M. D. Karvelis, Nucl. Phys. 47, 521 (1963).
- ²⁷M. Hyakutake *et al.*, J. Nucl. Sci. Technol. 11, 407 (1974).
- ²⁸J. P. Jeukenne, A. Lejeune, and C. Mahaux, Phys. Rev. C 16, 80 (1977).
- ²⁹F. A. Brieva and J. R. Rook, Nucl. Phys. A291, 317 (1977).
- ³⁰W. T. H. Van Oers and H. Haw, Phys. Lett. 45B, 227 (1973).
- ³¹I. Abdul-Jalil and D. F. Jackson, J. Phys. G 5, 1699 (1979).
- ³²C. Mahaux, in *Proceedings of the Conference on Microscopic Optical Potentials, Hamburg, 1978, Lecture Notes in Physics*, edited by H. V. von Geramb (Springer, Berlin, 1979), Vol. 89, p. 1.
- ³³W. D. Harrison and B. A. Whitehead, Phys. Rev. 132, 2607 (1963).
- ³⁴W. W. Daehnick and R. Sherr, Phys. Rev. 133, B934 (1964).
- ³⁵L. F. Hansen, S. M. Grimes, J. L. Kammerdiener, and V. A. Madsen, Phys. Rev. C 8, 2072 (1973).
- ³⁶H. R. Hiddleston, J. A. Aymar, and S. E. Darden, Nucl. Phys. A242, 323 (1975).
- ³⁷J. Rapaport, Phys. Lett. 92B, 233 (1980).
- ³⁸F. M. Mann, Hanford Engineering Development Laboratory Report No. HEDL-TME 78-83 UC-79d, 1979.
- ³⁹*Table of Isotopes*, 7th ed., edited by C. M. Lederer and V. S. Shirley (Wiley, New York, 1978).
- ⁴⁰H. Gruppelaar and G. Reffo, Nucl. Sci. Eng. 62, 756 (1977).
- ⁴¹B. Zwieglinski, J. Piotrowski, A. Saganek, and L. Sledzinska, Nucl. Phys. A209, 348 (1973).